

Optical study of poly(vinyl alcohol)/hydroxypropyl methylcellulose blends

Osiris W. Guirguis · Manal T. H. Moselhey

Received: 1 March 2011 / Accepted: 4 April 2011 / Published online: 26 April 2011
© Springer Science+Business Media, LLC 2011

Abstract The proposal in this study was to evaluate the optical properties of different biopolymers films. The materials used were poly(vinyl alcohol) (PVA) and hydroxypropyl methylcellulose (HPMC). PVA/HPMC blends were prepared by casting technique. Variations in the group coordination in the infrared region were followed. The effects of HPMC concentrations on the optical properties of the PVA films were studied by near infrared, ultraviolet/visible, transmittance, and reflectance in the spectral region 200–2500 nm. Absorption, transmittance, and reflectance spectra were used for the determination of the optical constants. The study has been also extended to include the changes in the optical parameters including the band tail width and band gap energies and extinction coefficient for the investigated films. The results indicate that the optical band gap was derived from Tauc's extrapolation and decreases with the HPMC contents. The obtained optical parameters were found to be strongly affected by HPMC contents.

Introduction

The categories of materials that are used as biomaterials include metals, ceramics, carbons, glasses, modified natural biomolecules, synthetic polymers, and composites consisting of various combinations of these material types [1].

The physical properties of polymers may be affected by doping. A graft copolymer is a type of branched copolymer

with the side chain being different and separate from the main chain. Detailed studies of doped polymer with different dopant concentrations allow the possibility of choice of the desired properties [2, 3].

Poly(vinyl alcohol) (PVA) is unique among polymers (chemical compounds made up of large, multiple-unit molecules) in that it is not built up in polymerization reactions from single-unit precursor molecules known as monomers. The chemical structure of the vinyl alcohol repeating units is: $(-[-\text{CH}_2-\text{CHOH}-]_n-)$ [4]. PVA is a water-soluble poly-hydroxy polymer, one of the few linear, no halogenated aliphatic polymers. PVA has a two dimensional hydrogen-bonded network sheet structure. The physical and chemical properties of PVA depend to a great extent on its method of preparation.

The PVA is an important material regarding its large scale applications. It is used in surgical devices, sutures, hybrid islet transplantation, implantation, blend membrane [5], and in synthetic cartilage in reconstructive joint surgery [6]. A new type of soft contact lens was developed from PVA hydrogel prepared by low temperature crystallization technique [7]. PVA is also used in sheets to make bags for premeasured soap, for washing machines, or to make longer bags used in hospitals [8]. PVA was selected as the hydrogel component based on its favorable water-soluble, desirable physicochemical properties, and its biocompatibility [9]. Furthermore, chemically crosslinked PVA hydrogel has been gaining increasing attention in the field of biomedics [10].

Hydroxypropyl methylcellulose (HPMC) belongs to the group of cellulose ethers which has been used already for a year by paper of conservators as glue and sizing material. The material is soluble in water as well as in polar organic solvents (makes it possible to combine aqueous and non aqueous conservation methods) [11].

O. W. Guirguis (✉) · M. T. H. Moselhey
Biophysics Department, Faculty of Science, Cairo University,
Giza 12613, Egypt
e-mail: osiris_wgr@yahoo.com

The amalgamation of polymer and pharmaceutical sciences led to the introduction of polymer in the design and development of drug delivery systems. Polysaccharides fabricated into hydrophilic matrices remain popular biomaterials for controlled-release dosage forms, and the most abundant naturally occurring biopolymer is cellulose; so HPMC, hydroxypropyl cellulose, microcrystalline cellulose, and hydroxyethyl cellulose can be used for production of time-controlled delivery systems [12]. Targeting of drugs to the colon following oral administration has also been accomplished by using polysaccharides such as HPMC and in hydrated form [12].

Most novel capsule materials are based on water-soluble cellulose derivatives such as methylcellulose and HPMC [13]. It was reported that the dissolution of HPMC capsules in water or gastric fluids at 37 °C was only slightly longer than that of gelatin capsules [13].

In this study, a trail will be carried out to produce the best product of PVA/HPMC blend and also to overcome the defects of the individual homopolymers (PVA and HPMC). Variations in the group coordination in the infrared region were followed. The effects of HPMC concentrations on the optical properties of the PVA films were studied by performing UV/VIS/near infrared (NIR) analysis which gives an evidence for understanding energy band diagram and optical parameters which is relatively affected by processing conditions. The study has been also extended to calculate the extinction coefficient (K) for the investigated films.

Experimental

Materials and sample preparation

The PVA granules with molecular weight of 125 kg/mol were supplied from El-Nasr Company, Cairo, Egypt. Hydroxypropyl methylcellulose (HPMC; Pharmacoat 606) with molecular weight of 133.4 kg/mol was supplied by Shin Etsu Chemical Co., Japan.

The solution method [14] was used to obtain film samples. This method depends on the dissolution, separately, the weighted amounts of PVA granules and HPMC powder in double-distilled water. Complete dissolution was obtained using a magnetic stirrer in a 50 °C water bath.

To prepare thin films of the homopolymers (PVA and HPMC) and the blend of their samples (PVA/HPMC) with different weight percentages 100/0, 90/10, 75/25, 50/50, 25/75, and 0/100 wt/wt%, the solutions were mixed together at 50 °C with a magnetic stirrer. Thin films of appropriate thickness (about 0.01 cm) were cast onto stainless steel petri dishes (10 cm diameter). The prepared films were kept at room temperature (about 25 °C) for

7 days until the solvent completely evaporated and then kept in desiccators containing fused calcium chloride to avoid moisture. The samples were measured at room temperature as solid films (slabs) of dimensions 1 × 4 cm.

Fourier transform infrared (FTIR) spectroscopy

The FTIR absorption spectra of the prepared films under investigations were performed over the range 4000–400 cm^{-1} using a Bruker Vector 22 Spectrophotometer (Germany) with accuracy better than $\pm 1\%$.

UV/VIS/NIR spectroscopic measurements

The measurements in the ultraviolet region from 200 to 400 nm, visible region from 400 to 700 nm, and NIR region from 900 to 2500 nm for PVA, HPMC, and PVA/HPMC, respectively, blends were carried out using a Shimadzu (UV/VIS/NIR) Double Beam Spectrophotometer with standard illuminant C (1174.83), has a serial number B44360512, Model V-530 and band width 2.0 nm covers the range 200–2500 nm with accuracy $\pm 0.05\%$.

Theoretical background

Optical parameters

The absorption coefficient (α) of the present materials strongly depends on optical transmission, reflection, and thickness of film which is evaluated using the relation [15, 16]:

$$\alpha = [\ln(1 - R)/T]^2/d, \quad (1)$$

where T is the transmittance and d is the thickness of the sample in cm (the reflectance, R is neglected in this calculation).

The optical energy gap (E_g) of the thin films has been determined from absorption coefficient data as a function of photon energy ($h\nu$ in eV). According to the generally accepted model proposed by Tauc for higher values of absorption coefficient where the absorption is associated with interband transitions, it yields the power part which obeys the Tauc [17] and Mott and Davis [18] relation as:

$$\alpha h\nu = B(h\nu - E_g)^n, \quad (2)$$

where B is the slope of the Tauc edge called the band tail parameter and n is the type of electronic transition responsible for absorption, being 0.5 for direct transition and 2 for indirect one.

In the low absorption region, the absorption coefficient (α) shows an exponential dependence on photon energy ($h\nu$) and obeys the Urbach relation [15]:

$$\alpha = \alpha_0 \exp(h\nu/E_b), \tag{3}$$

where α_0 is a constant and E_b is the Urbach energy, interpreted as the width of the tails of localized states in the band gap.

The absorption edge (E_c), the band tail (E_b), the direct energy gap (E_d), and the indirect energy gap (E_{ind}) were also calculated from the graphs of: α versus $h\nu$, $\ln \alpha$ versus $h\nu$, $(\alpha h\nu)^2$ versus $h\nu$, and $(\alpha h\nu)^{1/2}$ versus $h\nu$, respectively.

The extinction coefficient (K) is important parameters characterizing photonic materials. Value of K can be calculated from transmission and reflection spectra using the relation [16]:

$$K = \alpha\lambda/4\pi, \tag{4}$$

where λ is the wavelength and α is the absorption coefficient. The decrease in the extinction coefficient with an increase in wavelength shows that the fraction of light lost due to scattering.

Color parameters

The relative brightness values (y_r), the brightness (L), the color constants (A) and (B), the whiteness index (W), the yellowness index (Y_e), the color difference (ΔE), the chroma (ΔC), and the hue (ΔH) are estimated using the CIE relations as follows [19, 20]:

$$L = 10\sqrt{y} \tag{5}$$

$$A = 17.5 \frac{[(x/0.9804) - y]}{\sqrt{y}} \tag{6}$$

$$B = 7 \frac{[y - (z/1.181031)]}{\sqrt{y}} \tag{7}$$

$$W = 4[(z/1.181031) - 3y] \tag{8}$$

$$Y_e = 125 \frac{[(x/0.9804) - (z/1.181031)]}{y} \tag{9}$$

and

$$\Delta E = \sqrt{(\Delta L)^2 + (\Delta A)^2 + (\Delta B)^2}, \tag{10}$$

where x , y , and z are the tristimulus values and,

$$\Delta L = L(\text{PVA/HPMC}) - L(\text{pure PVA})$$

$$\Delta A = A(\text{PVA/HPMC}) - A(\text{pure PVA})$$

$$\Delta B = B(\text{PVA/HPMC}) - B(\text{PVA}).$$

The chroma and hue are given by:

$$\Delta C = \sqrt{A_{\text{PVA/HPMC}}^2 + B_{\text{PVA/HPMC}}^2} - \sqrt{A_{\text{purePVA}}^2 + B_{\text{purePVA}}^2} \tag{11}$$

and

$$\Delta H = \sqrt{(\Delta E)^2 - (\Delta L)^2 - (\Delta C)^2}. \tag{12}$$

Results and discussions

Characterization of PVA/HPMC blends

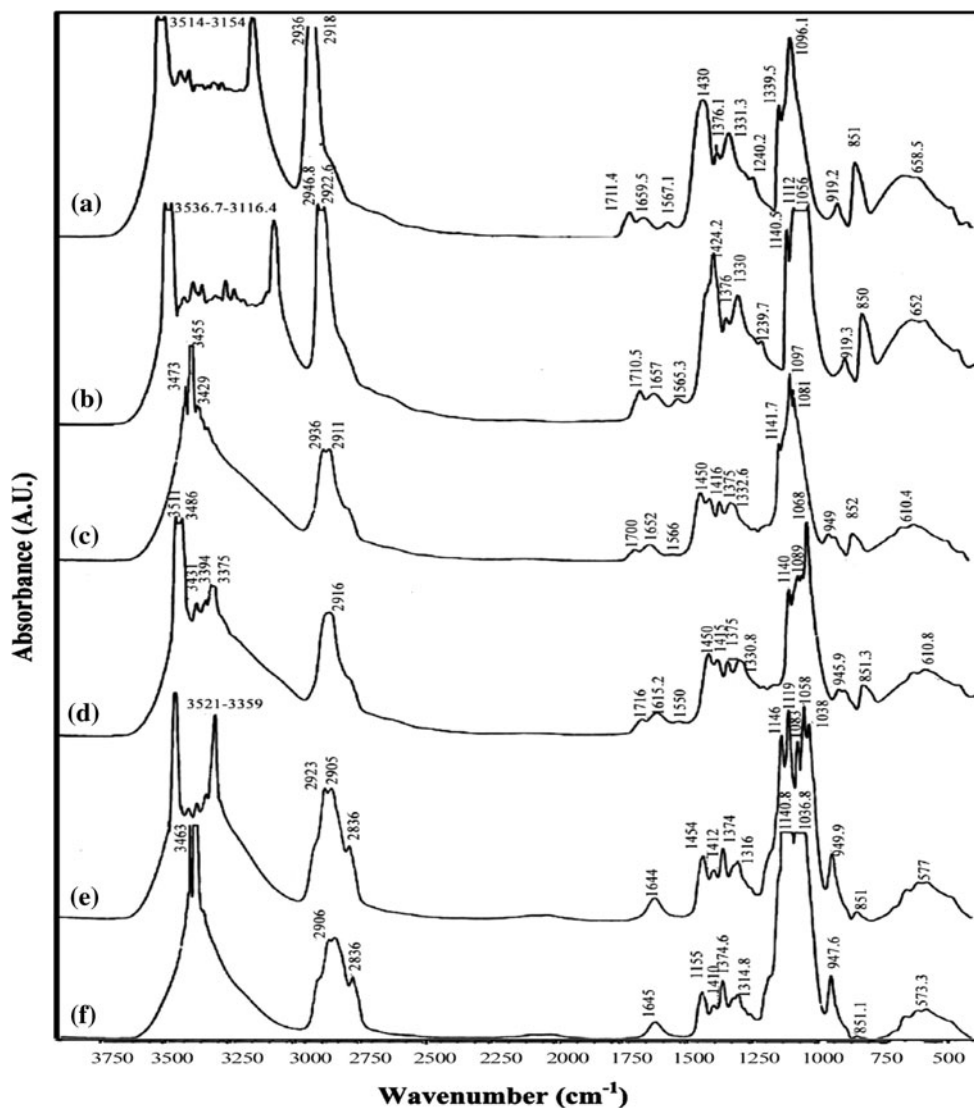
FTIR spectral analysis

Figure 1 shows the FTIR absorbance spectra for PVA/HPMC blended samples as functions of wavenumber in the range 4000–600 cm^{-1} . The chemical assignments were considered and are shown in Table 1. The spectrum of PVA seems to be consistent with that previously reported in the literatures [14, 21]. Amorphous and crystalline phases show partly resolved absorption in the 1150–1000 cm^{-1} region. It is clear from the figure and the table for PVA (curve a) that a relatively broad and intense $\nu(\text{OH})$ absorption stretching band is observed between 3515 and 3154 cm^{-1} indicating the presence of a polymeric association of the free hydroxyl group and bonded OH-stretching vibration [22, 23]. This broad and intense band usually occurs along with sharp less intense “monomeric” and “dimeric” OH absorption. Also, two distinct absorption bands occurring at 2936 and 2918 cm^{-1} result from antisymmetric $\nu_{as}(\text{CH}_2)$ and symmetric $\nu_s(\text{CH}_2)$ stretching vibrations, respectively.

The bands at 1712 and 1567 cm^{-1} of the carbonyl group are due to absorption of the residual acetate group [4]. The band at 1712 cm^{-1} was assigned to “free” unassociated and to associated hydrogen-bonded carbonyl group in the sample [24]. The band at 1659 cm^{-1} was attributed to the absorption of H_2O [25]. The symmetric bending mode $\nu_s(\text{CH}_2)$ is found at 1430 cm^{-1} . In addition, the bands at 1376 and 1240 cm^{-1} result from rocking methyl groups (CH_3) or wagging vibrations of CH_2 and CH , respectively. The band at about 1331 cm^{-1} is assigned to mixed $\nu_s(\text{CH}$ and $\text{OH})$ bending modes and is attributed to the associated alcohols.

The stretching band at 1140 cm^{-1} is known to be the crystallization-sensitive band of PVA and is taken as a measure of the degree of crystallinity. It is believed that this band arises from the symmetric $\nu(\text{C}-\text{C})$ stretching mode related to the regular repetition of the trans-configuration of the zigzag chain in a crystalline region. In addition, it is inferred that the 1140 cm^{-1} band might be due to a kind of absorption mechanism related to the presence of the oxygen atom. The band at about 1096 cm^{-1} is assigned to $\nu(\text{C}-\text{O})$ stretching vibration of ether group. The band at 919 cm^{-1} is related to syndiotactic structure and is assigned to the $\nu_t(\text{CH}_2)$ rocking vibration. The bands at 851 cm^{-1} are assigned to $-\text{CH}_2$

Fig. 1 Variation in FTIR spectra of PVA/HPMC blends: (a) 100/0, (b) 90/10, (c) 75/25, (d) 50/50, (e) 25/75, and (f) 0/100 (wt/wt%)



rocking vibration and at 607 cm^{-1} due to O–H twisting [25].

On the other hand, the FTIR spectrum of the most evident absorption bands for HPMC (curve f) is also illustrated in Table 1. The broadness band observed between 3553 and 3360 cm^{-1} may be due to the free hydroxyl group and hydrogen-bonded OH-stretching vibration. In addition, three absorption bands occurring at 2936 , 2907 , and 2836 cm^{-1} results from the antisymmetric stretching band of CH_2 or CH_3 group. No significant absorption until about 1648 cm^{-1} which may be due to C=O stretching mode appears. The bands at 1456 cm^{-1} is probably due to CH_2 deformation while the bands existing at 1411 and 1375 cm^{-1} are due to bending vibration mode $\nu_\delta(\text{CH})$ of CH_2 . The relatively intense band at 1141 cm^{-1} is related to the symmetric $\nu_s(\text{C}-\text{O})$ stretching while the bands at 1087 cm^{-1} are due to the symmetric $\nu_s(\text{C}-\text{O})$ stretching vibration. The band at 948 cm^{-1} is due to C–O deformation

while the small absorption band at 851 cm^{-1} may be due to the CH_2 rocking vibration and at 610 cm^{-1} due to O–H twisting.

From the obtained data of PVA/HPMC blend samples illustrated in Fig. 1 and Table 1, it is clear that:

- The absorbance band observed at $3515\text{--}3154\text{ cm}^{-1}$ in pure PVA becomes sharp by adding different concentrations of HPMC.
- The strong band at 2936 cm^{-1} associated with C–H stretching vibration of pure PVA shows shift in its position and decrease in its intensity by adding different concentrations of HPMC and increase in its intensity at only 10 wt% HPMC sample.
- The band at 1712 cm^{-1} of pure PVA shows little shifts in its position and intensity by adding different concentrations of HPMC and completely disappeared at concentrations 75 and 100 wt% HPMC.

Table 1 Positions and assignments of the most absorption bands of PVA/HPMC blends

Wavenumber (cm ⁻¹)						Assignments
PVA/HPMC blend (wt/wt%)						
0/100	90/10	75/25	50/50	25/75	0/100	
3515–3154	3537–3116	3473–3430	3533–3375	3553–3360	3553–3360	Hydrogen bonded and hydroxyl O–H group
2936	2947	2934	2936	2932	2936	CH ₂ or CH ₃ stretching vibration
2918	2923	2911	2916	2906	2907	C–H stretching vibration
–	–	–	2833	2837	2836	C–H stretching vibration
1712	1711	1700	1716	–	–	Carbonyl group C=O stretching
1660	1658	1653	1651	1645	1648	Water absorption and C=O stretching
1567	1565	1566	–	–	–	Carbonyl group C=O stretching
1430	1424	1450	1450	1454	1456	O–H, C–H bending and –CH ₂ deformation
–	–	1416	1415	1413	1411	Bending vibration mode of CH ₂
1376	1376	1376	1375	1375	1375	–CH ₂ wagging
1331	1331	1333	1331	1317	1315	C–H and O–H bending
1240	1240	1200 shoulder	–	–	–	O–H bending and C–H wagging
1140	1140	1142	1140	1146	1141	C–O stretching vibration
–	1113	–	1114	1119	–	C–O stretching vibration
1096	1087	1082	1088	1083	1087	C–O stretching vibration
919	919	946	946	948	948	C–O deformation and CH ₂ rocking
851	851	852	851	851	851	Skeletal and CH ₂ rocking
607	617	617	611	617	617	O–H twisting

- The band at 1659 cm⁻¹ of pure PVA shift in its position and its intensity decreased with increasing HPMC concentration.
- The band at 1567 cm⁻¹ of pure PVA shows little shift in its position and decreased in its intensity by increasing HPMC concentration and disappeared at concentration 75 wt% HPMC.
- The bands at 1430, 1376, and 1331 cm⁻¹ of pure PVA shift in their positions and variation in their intensities with increasing HPMC concentration.

By following the FTIR spectra, it is easily assigned the observed strong band as OH-stretching vibration. The variation of this band intensity with increasing HPMC contents may have allowed us to specify a strong or weak interaction between HPMC ions and the O–H stretching groups belonging to different chains in PVA [4, 14].

The FTIR spectra shown in Fig. 1 were completely absorbed in the OH stretching for all the samples. Moreover, O–H groups are polar groups, and the accessibility for polar groups is of great importance in polymer modification (especially in fabrication). The position and the bonding of these groups are influenced by crystallinity and crystal modification. Furthermore, the increase in absorbance of carbonyl groups indicates decrease in their growth, which may suggest that they are converted into volatile compounds [24]. A decrease in carbonyl groups

can be related to enhancement of some mechanical properties of the polymers. The shape of the carbonyl band at 1712 cm⁻¹ indicated a change in the balance of free and associated carbonyl groups in the blends. The hydroxyl and carbonyl stretching vibration bands are affected by hydrogen bonding interactions and are most amenable to quantitative analysis.

The heights of the peaks of the assigned groups at their wavenumbers shown in the spectra were taken to represent the variation in the group band intensities for different HPMC concentrations (Fig. 2). A clear deviation was observed in the absorption bands of the PVA/HPMC copolymers when compared with that detected for pure PVA. Any increase or decrease means a change in the molecular configuration of the polymer.

As shown by the FTIR results, it was clear that an increase in the concentration of HPMC changed the chemical bonds and hence changed the molecular configuration of PVA which is shown by the pronounced variation in the intensity of absorbance bands and little shifts in band positions. The change in intensity and disappearance of some spectral bands associated with infrared active groups of the polymer (PVA and HPMC) may be attributed to the fact that in the polymeric materials that contain two or more components, the resulting spectrum is approximately the sum of these components. In addition, the

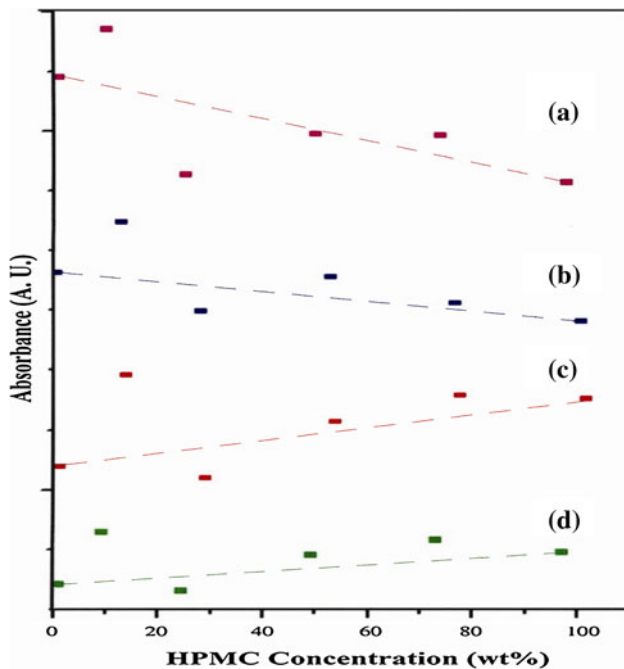


Fig. 2 Variation in band intensities for some chemical groups of PVA/HPMC blends as functions of HPMC concentration at: (a) 2942–2932 cm^{-1} , (b) 1331–1327 cm^{-1} , (c) 1144–1134 cm^{-1} , and (d) 949–919 cm^{-1}

change in the spectral position of some bands of PVA after the additions of different HPMC concentrations may be attributed to some of the monomer units of PVA are sensitive to their environment. Shifts in bands positions in the spectra of the copolymer are observed as opposed to homopolymers [25].

It is known that the type of bonding in the network structure plays a dominant role in deciding the rigidity of the structure and also associated with the change in cross-linkage and coordination of the polymer network [26].

The stretching force constant (F) in Newton and the local bond length in nm were also calculated from the following equations:

$$F = [2\pi cv]^2 \cdot \mu, \quad (13)$$

where c is the speed of light, v is the frequency in Hz, and μ is the reduced mass given by:

$$\mu = [(Z_a/N_A)(Z_b/N_A)] / [(Z_a/N_A) + (Z_b/N_A)], \quad (14)$$

where N_A is the Avogadro's number, Z_a and Z_b are the atomic number of the atoms, respectively, which form the bond. In case of double bond, Eq. 2 is divided by 2. Therefore, the bond length is given by [27, 28]:

$$\text{Bond length} = \left\{ (X_a \cdot X_b)^{3/4} / [(F - 30) / (5.28 \cdot O)] \right\}^{2/3}, \quad (15)$$

where X_a and X_b are the electronegativity of the atoms, respectively, which share in the bond length, O is the bond order (for single bond $O = 1$, while for double bond $O = 2$), and F is the stretching force.

Table 2 shows the stretching force and the bond length for the effective band frequencies of O–H, C–H, C=O, and CH_2 of PVA/HPMC-blended samples. It is noticed that there are changes in both stretching force and bond length. The presence of hydrogen in bonded structures in some polymers can be inferred at once from the presence of the bond form of the hydrogen stretching mode.

It is clear from the table in calculation of bond length that [27]:

- Hydroxyl O–H group decreased as the concentration increases which indicated that increase in elastic moduli.
- C=O stretching group bond length increases as the concentration increases which means that the elastic moduli decreases by increasing the concentration.
- C–H bending group remains the same by increasing the concentration.
- For $-\text{CH}_2$ rocking group the bond length decreased as the concentration increased which indicated that increase in elastic moduli.

NIR spectral analysis

The absorbance spectra and the assignments of the most important absorbance bands in the NIR region (900–2500 nm) for PVA/HPMC-blended samples are shown in Fig. 3. Table 3 illustrates the variation of the peak position while Table 4 represents the change in the area of each peak, the band width, and the absorbance values of some bands as well as the bond vibration and structure for PVA/HPMC-blended samples. It is clear from Fig. 3 and Table 3 for PVA/HPMC-blended samples that [29]:

- The band at 2410 nm appeared only in pure PVA and 10 wt% HPMC-doped sample and also, the band at 2471 nm for pure HPMC. The two bands disappeared completely for all other doping concentrations (25, 50, and 75 wt% HPMC).
- The band at 2310 nm for pure PVA shifted toward lower wavelengths by increasing HPMC concentration up to 50/wt% and then disappeared for 25/75 wt/wt% PVA/HPMC blend sample and for also pure HPMC.
- The band at 2274 nm for pure HPMC only appeared for PVA/HPMC (25/75 wt/wt%) blend sample, while disappeared with concentrations (10, 25, and 50 wt% HPMC) as well as pure PVA.

Table 2 The stretching force and the bond length for PVA/HPMC blends

PVA/HPMC (wt/wt%)	Wavenumber (cm ⁻¹)	Reducing mass (kg)	Stretching force (N)	Bond length (nm)
<i>Hydroxyl (O–H) group</i>				
100/0	3334	1.57×10^{-27}	620.49	0.1185
90/10	3327	1.57×10^{-27}	617.61	0.1184
75/25	3451	1.57×10^{-27}	664.85	0.113
50/50	3454	1.57×10^{-27}	665.82	0.1128
25/75	3451	1.57×10^{-27}	664.72	0.1128
0/100	3467	1.57×10^{-27}	670.90	0.1122
<i>C=O stretching group</i>				
100/0	1660	1.14×10^{-26}	556.06	0.218
90/10	1658	1.14×10^{-26}	554.85	0.219
75/25	1653	1.14×10^{-26}	551.48	0.220
50/50	1651	1.14×10^{-26}	550.47	0.2203
25/75	1645	1.14×10^{-26}	546.25	0.2215
0/100	1698	1.14×10^{-26}	546.46	0.222
<i>C–H bending group</i>				
100/0	1430	1.54×10^{-27}	111.97	0.380
90/10	1424	1.54×10^{-27}	111.02	0.383
75/25	1416	1.54×10^{-27}	109.81	0.387
50/50	1415	1.54×10^{-27}	109.58	0.388
25/75	1413	1.54×10^{-27}	109.23	0.389
0/100	1411	1.54×10^{-27}	108.94	0.390
<i>Skeletal and –CH₂ rocking group</i>				
100/0	919	1.54×10^{-27}	92.49	0.456
90/10	919	1.54×10^{-27}	92.52	0.455
75/25	946	1.54×10^{-27}	98.002	0.431
50/50	946	1.54×10^{-27}	97.953	0.430
25/75	948	1.54×10^{-27}	98.34	0.4298
0/100	948	1.54×10^{-27}	98.30	0.4296

- The bands at 2208 nm for pure PVA and at 2211 nm for pure HPMC disappeared for all concentrations except for (25/75 wt/wt%) PVA/HPMC blend sample.
- The bands at 1780 and 1782 nm for pure PVA and pure HPMC, respectively, are shifted toward higher wavelengths with PVA/HPMC blend samples with different concentrations of HPMC.
- The band at 1752 nm for pure PVA disappeared by increasing HPMC concentration above 25 wt%.
- The band at 1724 nm for pure PVA appeared in the range (1710–1712 nm) by doping PVA with different concentrations of HPMC.
- At the peak position 2090 nm for ROH group: the area under the peak sharply decreased with increasing the concentration of HPMC toward the pure HPMC value.
- At the peak position 1940 nm for H₂O group: the behavior of the area is a fluctuated behavior between the values of the PVA and HPMC homopolymers.

Moreover, the variation in the intensity of the peaks means that there are changes in the molecular configuration as the dopant concentration changed. A clear variation was observed in the peak positions, and peak areas of the PVA/HPMC copolymers when compared with that shown for the homopolymer samples. In addition, it is noticed that strong local interaction between HPMC and other groups belonging to different chains in PVA will take place at the expense of the intermolecular interaction between these chains. This is in turn can be directly correlated with variations in the mechanical behavior of the polymer [30].

It is clear from Table 4 for PVA/HPMC blended samples that:

- At the peak position 2352 nm for HC=CHCH₂ group: the area under the peak increases first and then decreases up to 50 wt% HPMC, then increases again but still with value less than that of the pure PVA and higher than that of pure HPMC.

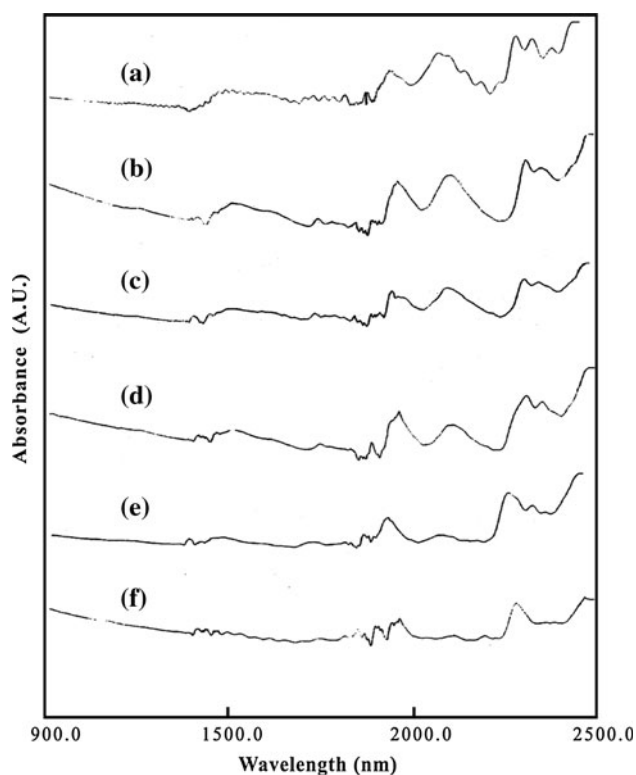


Fig. 3 Variation in NIR spectra of PVA/HPMC blends: (a) 100/0, (b) 90/10, (c) 75/25, (d) 50/50, (e) 25/75, and (f) 0/100 (wt/wt%)

Electronic absorption (UV/VIS) analysis

The study of optical absorption spectra provides essential information about the band structure and the energy gap in crystalline and non-crystalline materials. Analysis of the absorption spectra in the lower energy part gives information

about atomic vibrations, while the higher energy part of the spectrum gives knowledge about electronic state in atoms. Hence, the study of optical properties in the UV/VIS regions can help in a better understanding of the electronic structure and optical material constants [31, 32].

Figure 4 shows the absorption spectra of both PVA and HPMC homopolymers as well as their blends in the wavelength range 200–700 nm. It is clear from the figure that the three curves are closed to each other in the visible region (400–700 nm). Sharp drops in the absorbance values were detected in the UV region (200–400 nm). The spectrum of pure PVA exhibits a shoulder like band at 280 nm which are related to high energy absorption. This band is assigned to the existence of carbonyl groups associated with ethylenic unsaturation of the type $[-(C=C)_n - C=O]$, $n = 2, 3$ [32]. The carbonyl groups may arise from charge-transfer reactions during polymerization with acetaldehyde, a hydrolysis of vinyl acetate or with the decomposition products a vinyl acetate-oxygen copolymer. The spectra are composed of an almost flat baseline (absorption negligible) and a step cutoff (big absorption). The absorbance values for both pure PVA and pure HPMC are lower than those for blend compositions in all wavelength range. Among these samples, the absorbance value for the blend sample of composition 25/75 wt/wt% PVA/HPMC is the highest one in the wavelength range 200–700 nm.

The variation in the absorbance values of the blend samples with increasing the concentration of HPMC may be attributed to the fact that increasing the dopant concentration decreases the transparency of the sample which may be due to that there is a change in the molecular configuration [33].

Table 3 Positions and assignments of the most NIR absorption bands of PVA/HPMC blends

Wavelength (nm)						Assignment	Chemical structure
PVA	10 wt% HPMC	25 wt% HPMC	50 wt% HPMC	75 wt% HPMC	HPMC		
2410	2410	–	–	–	2471	C–H stretching + C–C stretching	=CH group
2355	2353	2347	2350	2346	2345	C–H deformation – second overtone cellulose	HC=CHCH ₂
2308	2309	2309	2305	–	–	C–H stretching + C–H deformation	CH ₂ or CH ₃
–	–	–	–	2278	2274	O–H str. + O–H deformation	H ₂ O
2208	–	–	–	2190	2211	C–H stretching + C=O stretching	–CHO
2168	–	–	–	–	2181	=C–H stretching + C=O stretching	–CHO
2099	2094	2086	2094	2077	2095	O–H stretching + O–H deformation	ROH
1945	1940	1946	1939	1935	1939	O–H stretching + O–H deformation	H ₂ O
1815	1822	1823	1827	1826	1822	O–H stretching + 2(C–O) stretching	Cellulose
1780	–	1790	–	–	1782	C–H stretching first overtone	Cellulose
1752	1752	1755	–	–	–	C–H stretching first overtone	CH ₂
1724	1712	1739	1737	1723	–	C–H stretching first overtone	CH ₃ or CH ₂

Table 4 Variation of the peak position, the area under the peak and the band width for PVA/HPMC blends

PVA/HPMC blend (wt/wt%)	Peak position	Area under the peak	Band width (nm)	Absorbance	Assignment	Chemical structure
<i>For 2352 nm</i>						
100/0	2355	3.685	0.4	0.4395	C–H deformation – second overtone	HC=CHCH ₂
90/10	2353	4.394	0.4	0.4530		
75/25	2347	2.857	0.5	0.6190		
50/50	2350	2.413	0.7	0.6217		
25/50	2346	3.118	0.7	0.7552		
0/100	2345	1.583	0.8	0.2854		
<i>For 2090 nm</i>						
100/0	2099	10.787	0.9	0.3972	O–H stretching + O–H deformation	ROH
90/10	2094	6.411	0.7	0.4348		
75/25	2086	2.731	0.7	0.6070		
50/50	2094	0.991	0.7	0.5680		
25/50	2077	1.726	0.9	0.7990		
0/100	2095	0.597	0.7	0.2540		
<i>For 1940 nm</i>						
100/0	1945	4.367	0.7	0.3964	O–H stretching + O–H deformation	H ₂ O
90/10	1940	5.141	0.7	0.4180		
75/25	1946	3.140	0.3	0.5867		
50/50	1939	5.761	0.7	0.6010		
25/50	1935	4.193	0.6	0.7950		
0/100	1939	2.449	0.3	0.3296		

Optical parameters of PVA/HPMC blends

The total absorption spectral response (α) for PVA, HPMC, and their blends were calculated in the (UV/VIS) wavelength range from 200 to 700 nm and in the photon energy ranges 3.0–6.5 eV (UV region) and 2.0–3.2 eV (VIS region). Figure 5 shows the relation between the absorption

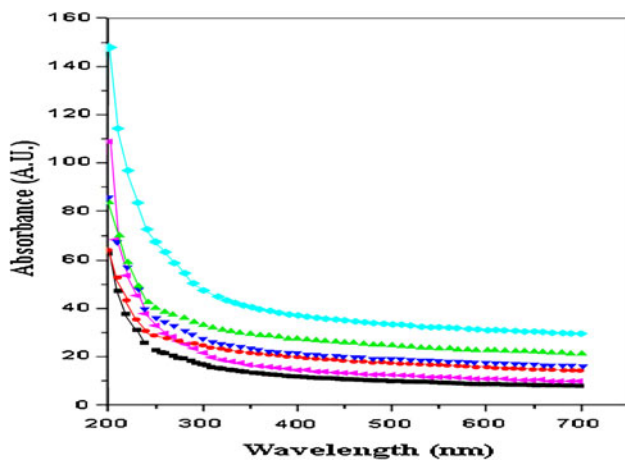


Fig. 4 The absorption spectra of PVA/HPMC blends: (filled square) 100/0, (filled circle) 90/10, (filled triangle) 75/25, (filled inverted triangle) 50/50, (filled diamond) 25/75, and (black left-pointing triangle) 0/100 (wt/wt%)

coefficients (α) as a function of wavelength in the UV range (200–400 nm) (a) and in the visible range (400–700 nm) (b) for PVA/HPMC-blended samples. It is clear from the figures that the absorption coefficient (α) increases gradually with increasing HPMC content up to 50 wt% HPMC and it decreases at concentration 75 wt% HPMC. The increase in α with the increase in the HPMC content may be attributed to the change of the molecular configuration which indicates to the formation of new color centers as previously mentioned and reported [14].

The fundamental absorption edge is one of the most important features of the absorption spectra of crystalline and amorphous materials. The increased absorption near the edge is caused by the transition of electrons from the valence band to the conduction band [33]. Figure 6 illustrates the plot of absorption coefficient against photon energy for PVA/HPMC blend samples in the ranges 3.0–6.5 eV (a) and 2.0–3.2 eV (b). It is clear that the absorption coefficient values (α) increases with increasing photon energy and exhibits a steep rise near the absorption edge and a straight line relationship is observed in the high α -region (in the UV region only). The intercept of extrapolation to zero absorption (i.e., $\alpha = 0$) with photon energy axis was taken as the value of absorption edge. The values obtained are listed in Table 5. It is clear that the values of the absorption edge (E_c) for dopant concentration

Fig. 5 The absorption coefficient (α) of PVA/HPMC blends as a function of wavelengths in the UV range 200–400 nm (a) and in the visible range 400–700 nm (b): (filled square) 100/0, (filled circle) 90/10, (filled triangle) 75/25, (filled inverted triangle) 50/50, (filled diamond) 25/75, and (black left-pointing triangle) 0/100 (wt/wt%)

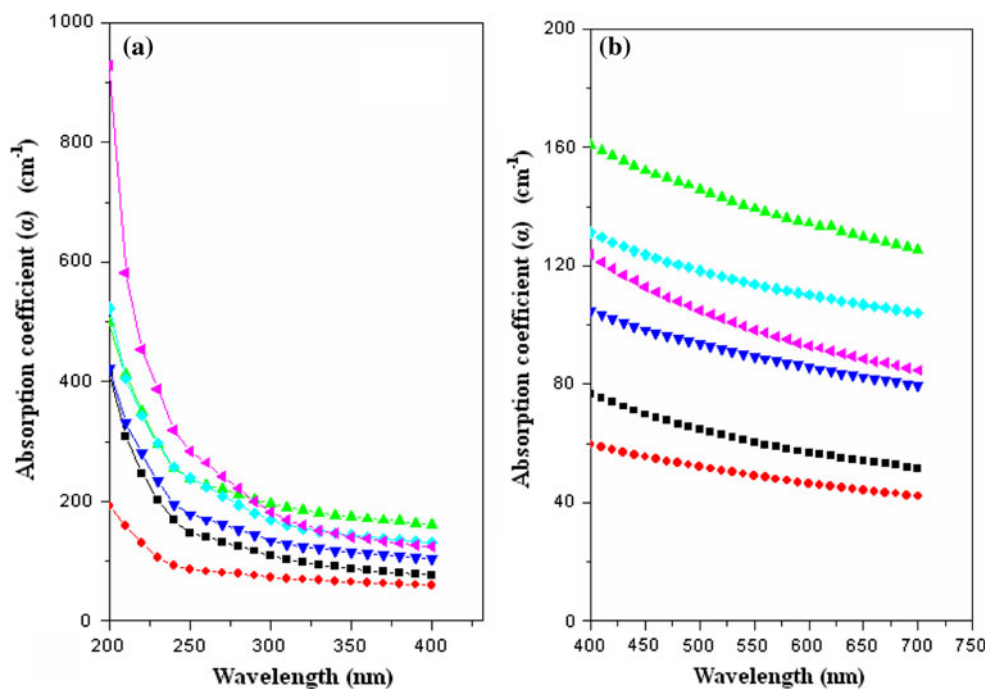
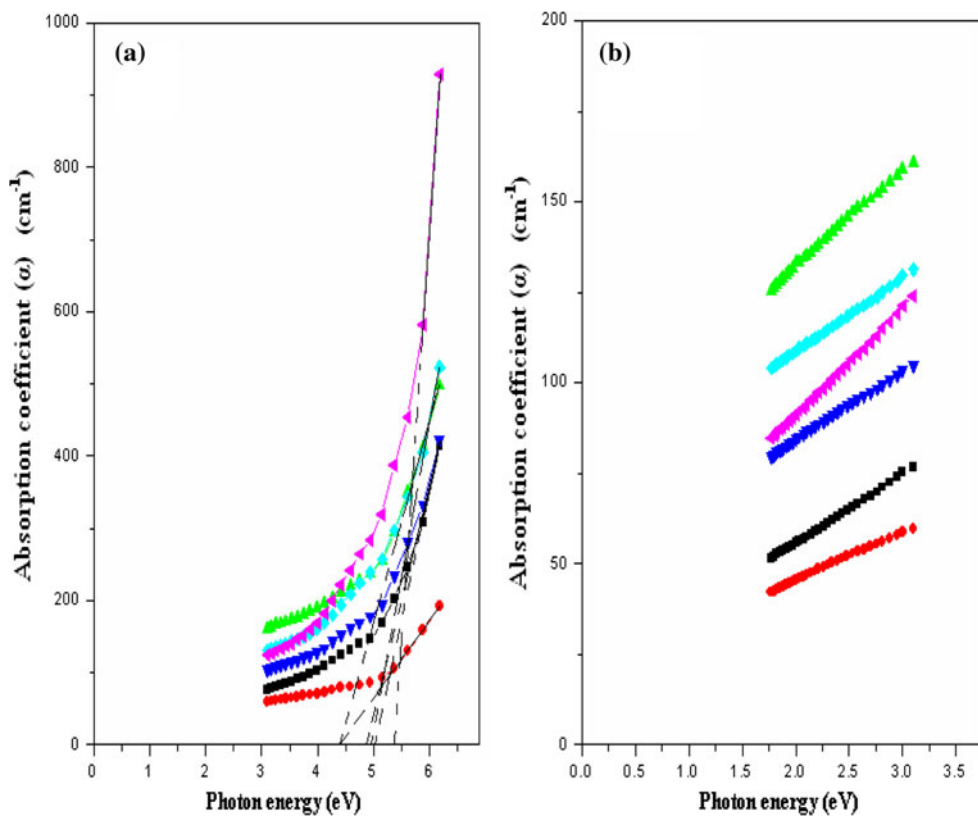


Fig. 6 The absorption coefficient (α) of PVA/HPMC blends as a function of photon energy ($h\nu$) in the UV range 3.0–6.5 eV (a) and in the visible range 2.0–3.2 eV (b): (filled square) 100/0, (filled circle) 90/10, (filled triangle) 75/25, (filled inverted triangle) 50/50, (filled diamond) 25/75, and (black left-pointing triangle) 0/100 (wt/wt%)



are lower than those for PVA and HPMC. This may reflect the induced changes in the number of available final states according to the blend composition.

Figure 7 shows the relation between $\ln \alpha$ and $h\nu$ for PVA/HPMC blended samples in the UV range 3.0–6.5 eV (a) and visible range 2.0–3.2 eV (b). The straight lines

Table 5 Values of absorption edge (E_e), band tail energy (E_b), direct energy gap (E_d), and indirect energy gap (E_{ind}) for PVA/HPMC blends

(a) In UV region (200–400 nm)				
PVA/HPMC blend (wt/wt%)	E_e (eV)	E_b (eV)	E_d (eV)	E_{ind} (eV)
100/0	5.00	0.368	5.09	4.25
90/10	4.40	0.206	3.60	3.50
75/25	4.40	0.186	5.05	3.59
50/50	4.86	0.232	5.09	4.14
25/75	4.95	0.237	5.35	4.00
0/100	5.36	0.362	5.65	4.82
(b) In the visible region (400–700 nm)				
PVA/HPMC blend (wt/wt%)	E_b (eV)	E_d (eV)		
1000/0	0.314	2.10		
90/10	0.295	2.04		
75/25	0.207	1.93		
50/50	0.228	2.00		
25/75	0.180	1.90		
0/100	0.299	2.10		

obtained suggest that the absorption follows the quadratic relation for interband transitions and the Urbach rule is obeyed [18]. The values of band tail energy (E_b) can be deduced from the slopes of the straight lines and are listed in Table 5. The E_b values decreases at 10 and 25 wt% HPMC and then increases by increasing the concentration of HPMC. These variations may be due to the variation in the internal fields associated with structure disorder in the system [18].

Figure 8 shows the dependence of $(\alpha hv)^2$ on hv for PVA/HPMC-blended samples. From the figure it is observed that the allowed direct energy gap (E_d) is determined by extrapolating the linear parts of the curves to zero absorption and the values are given in Table 5. It is clear that the values of E_d are close together and also with both of the pure samples.

Figure 9 shows the change of $(\alpha hv)^{1/2}$ as a function of hv for PVA/HPMC-blended samples. From the figure, the allowed indirect energy gap (E_{ind}) is determined by extrapolating the linear parts of the curves to zero absorption and the values of E_{ind} are represented in Table 5. It is clear that the values of E_{ind} are nearly close together and lie between 3.5 and 4.14 eV and still lower than those of both the pure samples. So the obtained values for E_{ind} show the dependence on the composition of the sample. It may be presumed that the variation of them may be due to the difference in the number of HPMC ions per unit length available for conduction and in addition the change in molecular configuration induced by dopant concentration.

It was noticed that the variation in the values of E_b , E_d , and E_{ind} with increasing the concentration of HPMC may be due to HPMC-induced structural changes in the system. In another meaning, this change may arise from the random fluctuations of the internal fields associated with the structure disorder in the amorphous region of polymer material. Furthermore, it was recognized that dopant plays a dominant role in morphological and microstructure changes occurring in the polymer matrix [14, 32].

Extinction coefficient

The extinction coefficient (K) describes the properties of the material to light of a given wavelength and indicates the amount of absorption loss when the electromagnetic wave propagates through the material, i.e., represents the damping of an EM wave inside the material. Figure 10 shows the variation in the extinction coefficient with wavelength of PVA/HPMC-blended samples. It is clear from the figure that similar behavior for all samples are observed and the values of K are found to be small in the order 10^{-4} throughout the studied wavelength range (200–700 nm) which indicate that the samples under investigation are considered to be insulating materials at room temperature [34]. In addition, the behavior of the absorption coefficient

Fig. 7 Urbach law plots for PVA/HPMC blends in the UV range (a) and visible range (b): (filled square) 100/0, (filled circle) 90/10, (filled diamond) 75/25, (filled inverted triangle) 50/50, (filled diamond) 25/75, and (black left-pointing triangle) 0/100 (wt/wt%)

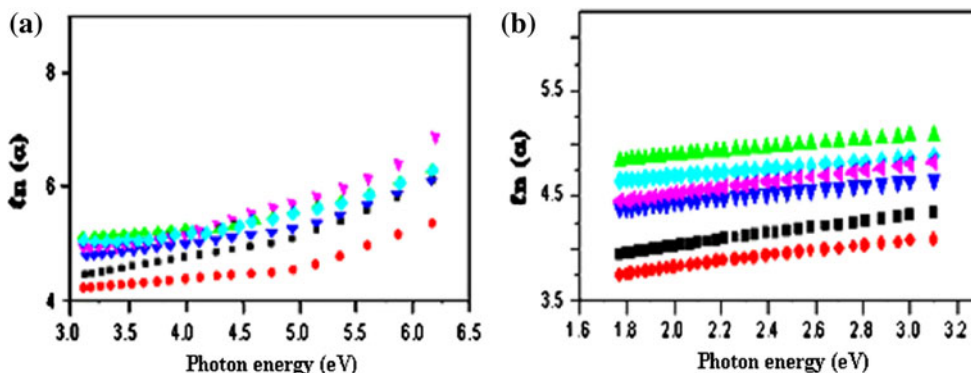


Fig. 8 The variation of $(\alpha h\nu)^2$ of PVA/HPMC blends as a function of photon energy ($h\nu$) in the UV range 3.0–6.5 eV (a) and in the visible range 2.0–3.2 eV (b): (filled square) 100/0, (filled circle) 90/10, (filled triangle) 75/25, (filled inverted triangle) 50/50, (filled diamond) 25/75, and (black left-pointing triangle) 0/100 (wt/wt%)

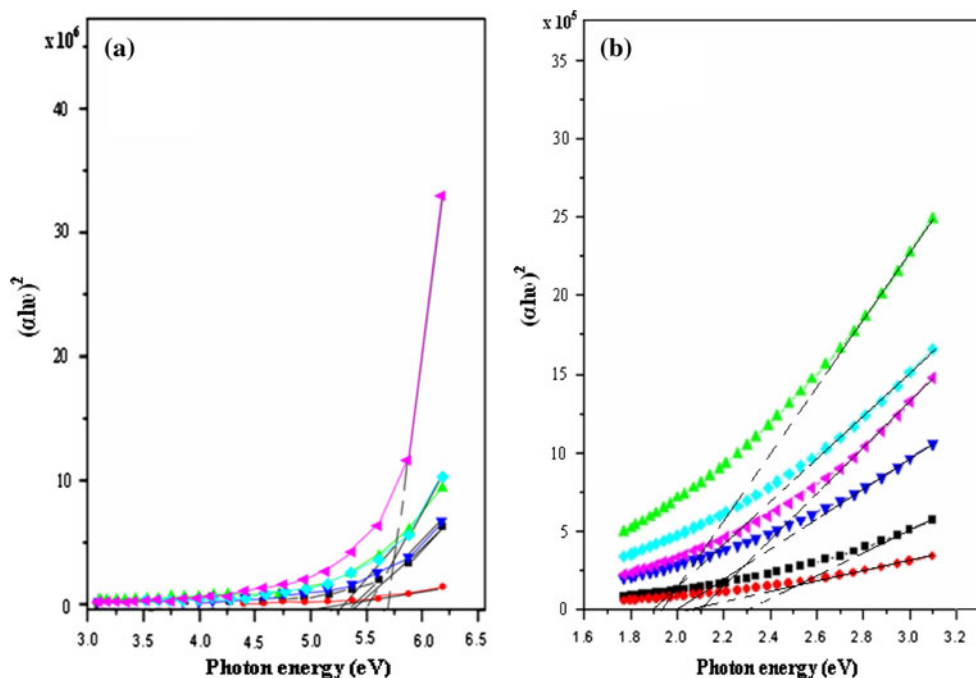
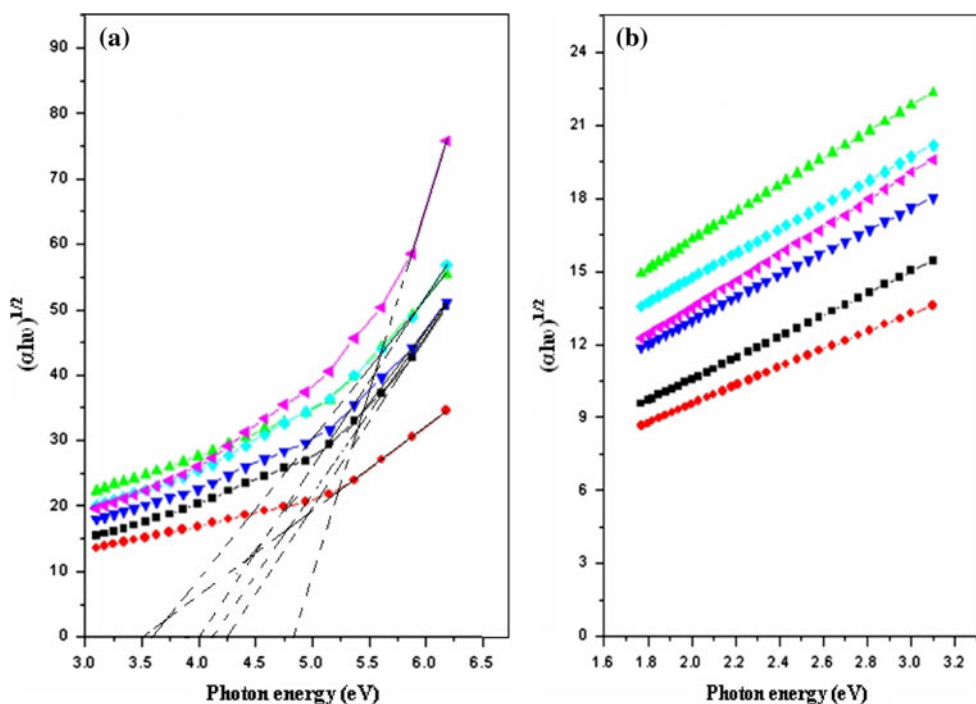


Fig. 9 The variation of $(\alpha h\nu)^{1/2}$ of PVA/HPMC blends as a function of photon energy ($h\nu$) in the UV range 3.0–6.5 eV (a) and in the visible range 2.0–3.2 eV (b): (filled square) 100/0, (filled circle) 90/10, (filled triangle) 75/25, (filled inverted triangle) 50/50, (filled diamond) 25/75, and (black left-pointing triangle) 0/100 (wt/wt%)



is preserved for all samples near the absorption edge. It is also clear that the blended sample 75/25 wt/wt% for PVA/HPMC indicates highest value of K through the whole range of wavelength (200–700 nm). Moreover, fluctuation behavior in the values of the extinction coefficient in the whole range of wavelength is observed around the PVA and HPMC homopolymers' values.

Optical reflectance and color difference calculations of PVA/HPMC blends

From the values of reflectance (figures are not shown for simplicity data). Table 6 illustrates the values of x_r , y_r , and z_r at peak positions for homopolymers and PVA/HPMC-blended samples.

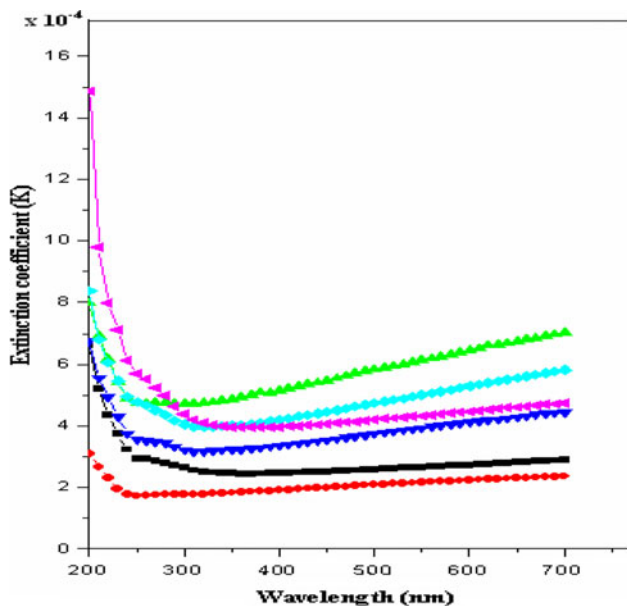


Fig. 10 Variation in the extinction coefficient (K) as a function of wavelength (λ) of PVA/HPMC blends: (filled square) 100/0, (filled circle) 90/10, (filled triangle) 75/25, (filled inverted triangle) 50/50, (filled diamond) 25/75, and (black left-pointing triangle) 0/100 (wt/wt%)

The relative brightness (y_r) is calculated and plotted as a function of wavelength (400–700 nm) and shown in Fig. 11 for PVA/HPMC-blended samples. It is observed from the figure that the behaviors of y_r for the samples are similar and no change in peak position (555.4 nm) is detected. It is also observed that for PVA/HPMC-blended samples, y_r changes irregularly and then sharply decreased at 75 wt% HPMC concentration (see the inset of Fig. 11).

Table 7 represents the variation of color parameters and their percentage changes calculated from the reflectance curves for PVA/HPMC blends. From the table it is observed that:

- The brightness (L):

The brightness (L) shows unremarkable increase with increasing the concentration of HPMC.

- The color constants A and B :

For PVA/HPMC blend samples, the values of color constants A and B show fluctuation in their behaviors by

Table 6 The x_r , y_r , and z_r tristimulus reflectance values of PVA/HPMC blends calculated from reflectance data

PVA/HPMC blend (wt/wt%)	x_r		y_r	z_r
	$\lambda = 446.8 \text{ nm}$	$\lambda = 587.5 \text{ nm}$	$\lambda = 555.4 \text{ nm}$	$\lambda = 450 \text{ nm}$
100/0	102	218	246	529
90/10	93	200	223	492
75/25	100	212	241	521
50/50	108	228	257	563
25/75	78	168	189	400
0/100	95	205	227	500

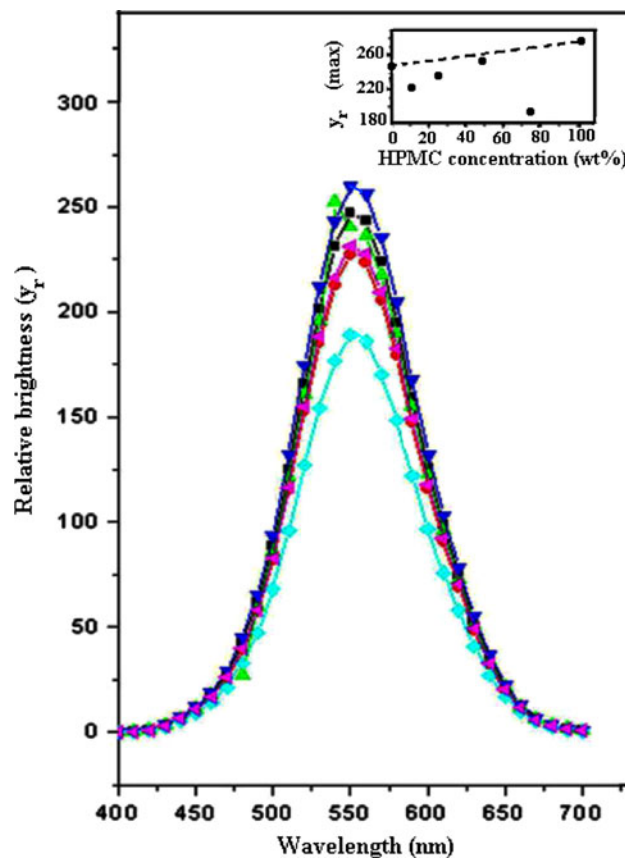


Fig. 11 Variation of the relative brightness value (y_r) with wavelength for PVA/HPMC blends: (filled square) 100/0, (filled circle) 90/10, (filled triangle) 75/25, (filled inverted triangle) 50/50, (filled diamond) 25/75, and (black left-pointing triangle) 0/100 (wt/wt%). The inset indicates the variation of the relative brightness value, y_r (max), as a function of HPMC concentration

increasing the concentration of HPMC, which indicates that there is variation in their color components with concentrations.

- The whiteness index (W):

The whiteness index (W) shows immeasurable change with increasing the concentration of HPMC.

- The yellowness index (Y_e):

Table 7 The results of color parameters changes and their percentage changes for PVA/HPMC blends

Color parameters	PVA/HPMC blend (wt/wt%)					
	100/0	90/10	75/25	50/50	25/75	0/100
<i>L</i>	5.5866	5.5848	5.6027	5.5839	5.5884	5.5893
$\Delta L\%$	–	–0.03%	0.29%	–0.05	0.03%	–
<i>A</i>	–0.1112	–0.1083	–0.1735	–0.1147	–0.0984	–0.1096
$\Delta A\%$	–	2.61%	–0.39%	–3.15%	11.51%	–
<i>B</i>	–0.1767	–0.1830	–0.1374	–0.1893	–0.1667	–0.1666
$\Delta B\%$	–	–3.57%	22.24%	–7.13%	5.72%	–
<i>W</i>	–2.4404	–2.4368	–2.4672	–2.434	–2.4452	–2.446
$\Delta W\%$	–	0.15%	–1.10%	0.26%	–0.20%	–
<i>Y_e</i>	–7.0891	–7.2539	–7.0589	–7.5369	–6.5642	–6.7222
$\Delta Y_e\%$	–	–2.32%	2.78%	–6.32%	7.40%	–
ΔE	–	0.0072	0.0754	0.0134	0.0164	–
ΔC	–	0.0038	0.0126	0.0126	–0.0152	–
ΔH	–	0.0083	0.0781	0.0186	2.239	–

The yellowness index (Y_e) values for PVA/HPMC blend samples decrease at 50 wt% and then increase at 75 wt%.

The obtained results indicate that variations in color difference between samples are occurred by the presence of HPMC by different concentrations with PVA.

The observed changes in the color parameters with the increase in the concentration of HPMC may be due to the change in the physical bonds and then changes in the molecular configuration of PVA as mentioned before which may lead to formation of new dopant centers of the polymeric material. In addition, the obtained results of the color parameters are of great importance for the improvement of the optical properties of the PVA.

Acknowledgements The authors are very grateful to the late Prof. Dr. El-Sayed A. Gaafar, Professor of Biophysics, Biophysics Department, Faculty of Science, Cairo University, Giza, Egypt, for his kind help to bring this study.

References

- Dumitriu S (1996) Polymeric biomaterials. Marcel Dekker Inc., New York
- Abdullah OG, Hussen SA (2010) International Conference on Manufacturing Science and Technology (ICMST), University of Sulaimani, Sulaimani
- Kulkarni RV, Sa B (2009) J Bioact Compat Pol 24:368
- Prichard GJ (1970) Poly(vinyl alcohol): basis principles and uses. Gordon and Breach, New York
- Saxena AK, Marler J, Benvenuto M, Willital GH, Vacanti JP (1999) Tissue Eng 5:525
- Peppas NA, Merrill EW (1977) J Biomed Mater Res 11:423
- Eaga CM, Kandukuri JM, Allenki V, Yamsani MR (2009) Der Pharm Lett 1:21
- Dumoulin MM, Carreau PJ, Utracki LA (1987) Polym Eng Sci 27:1627
- Zhang J, Yuan K, Wang Y, Zhang S, Zhang J (2007) J Bioact Compat Polym 22:207
- Kim SJ, Lee YM, Kim IY, Kim SI (2003) React Funct Polym 55:291
- Hofenk-de Graaff J (1981) Central research laboratory for objects of art and science. Gabriel Metsustraat and 1071 EA, Amsterdam, the Netherlands
- Kamel S, Ali N, Jahangir K, Shah SM, El-Gendy AA (2008) Express Polym Lett 2:758
- Leea C-Y, Chen G-L, Sheu M-T, Liu C-H (2006) Chin Pharm J 58:57
- El-Zaher NA, Osiris WG (2005) J Appl Polym Sci 96:1914
- Abd El-Raheem MM (2007) J Phys Condens Matter 19:216209
- Tintu R, Saurav K, Sulakshna K, Nampoorei VP, Radhakrishnan P, Thomas S (2010) J Non-Oxide Glasses 2:167
- Wood DL, Tauc J (1972) Phys Rev B 5:3144
- Mott NF, Davis EA (1979) Electronic processes in non-crystalline materials. Clarendon, Oxford
- CIE Recommendation on Colorimetry (1986) CIE Publ. No. 15.2. Central Bureau of the CIE, Vienna
- CIE Recommendation on Uniform Color Spaces (1971, 1978), Color difference equations, psychometric color terms, Suppl. No. 2 of CIE Publ. No. 15 (E-1.3.1), Paris
- Shiboyama M, Yamamoto T, Xiao C-F, Sakurai S, Hayami A, Nomura S (1991) Polymer 32:1010
- Sakellariou P, Hassan A, Rowe RC (1993) Polymer 34:1240
- Park CK, Choi MJ, Lee YM (1995) Polymer 37:1507
- Smith AL (1979) Applied infrared spectroscopy, fundamentals techniques and analytical problem-solving. Wiley, New York
- Desai RL, Shields JA (1969) Die Makromol Chem 122:134
- Bernard C, Chaussement S, Monteil A, Montagna M, Zampedri L, Ferrari M (2003) J Sol-Gel Sci Technol 26:925
- Gaafar MS, Marzouk SY (2007) Phys B Condens Matter 388:294
- Saddeek YB, Azooz MA, Kenawy SH (2005) Mater Chem Phys 94:213
- Osborne BG, Fearn T (1986) Near infrared spectroscopy in food analysis. Longman Scientific and Technical Groups. Wiley, New York

30. Tager A (1972) Physical chemistry of polymer. Mir Publishers, Moscow
31. Chikwenze RA, Nnabuchi MN (2010) Chalcogenide Lett 7:389
32. Abd El-Kader FH, Gafer SA, Basha AF, Bannan SI, Basha MAF (2010) J Appl Polym Sci 118:413
33. Miller A (1994) Handbook of optics, vol 1. McGraw-Hill, New York
34. Pankove JI (1975) Optical process in semiconductors. Devers Publication, New York